Estimating Particle-Size Distribution from Limited Soil Texture Data

T. H. Skaggs,* L. M. Arya, P. J. Shouse, and B. P. Mohanty

ABSTRACT

Particle-size distribution is a fundamental physical property of soils. Because particle-size data are frequently incomplete, it would be useful to have a method for inferring the complete particle-size distribution from limited data. We present a method for estimating the particle-size distribution from the clay (cl), silt (si), and fine plus very fine sand (fvfs) mass fractions (particle radii, *r*, between 25 and 125 μm). The method is easy to use, with the estimated distribution being given by a closed-form expression that is defined explicitly in terms of cl, si, and fvfs. The accuracy of the method is evaluated using particle-size data from 125 soils. The results show that the method should not be used when the silt fraction is greater than about 70%. For other soils, the estimated distribution agrees reasonably well with the true distribution, with the median level of accuracy being characterized by an average absolute deviation of 2% over 1 μm ≤ *r* ≤ 1000 μm, and a maximum absolute deviation of 9%.

Particle-size distribution is a basic physical property of mineral soils that affects many important soil attributes. Because particle-size distributions can be measured relatively easily and quickly, they have been used in the past as surrogate data for the indirect estimation of soil hydraulic properties (Arya et al., 1999, and references therein). Estimating hydraulic properties from particle-size data is particularly attractive when studying soil moisture at catchment or watershed scales because a detailed characterization of hydraulic properties is usually not feasible but particle-size data may be available from soil databases. Unfortunately, many databases do not contain the full particle-size distribution, but instead contain only the sand, silt, and clay mass fractions. The question arises: Is it possible to infer or estimate the full particle-size distribution from the percentages of sand, silt, and clay? This question has relevance in other contexts as well, such as when translating particle-size data from one classification system to another (Shirazi et al., 1988; Nemes et al., 1999).

One means of pursuing this question is suggested by models of fragmentation processes (Crawford et al., 1993; Turcotte, 1986). Fragmentation processes give rise to power-law particle-number distributions and (assuming uniform particle shape and density) power-law particle-size distributions. These distributions are linear under a log transformation, with the only unknown distribution parameter being contained in the slope of the line. If a soil has a power-law particle-size distribution, then a method for approximating the distribution from the sand, silt, and clay fractions is straightforward: the sand, silt, and clay fractions define two points on the log-transformed distribution from which the slope and unknown distribution parameter can be calculated. Other possible procedures for soils with power-law distributions can be derived using the concepts of fractals and self-similarity. Taguas et al. (1999) recently proposed one such method based on an iterated function system.

While these approaches seem promising in principle, theoretical (Tyler and Wheatcraft, 1992) and experimental (Kozak et al., 1996; Bittelli et al., 1999) evidence suggests that most soils do not follow a power-law distribution over the whole range of soil material. At best, power-laws hold only over subintervals of the distribution.

Although we omit the details here, we investigated variations on the simple power-law procedure suggested above, but were unable to devise a method that produced reasonable estimates from the sand, silt, and clay fractions. Taguas et al. (1999) concluded similarly that their method performed poorly when estimates were based on these three separates. If it is not possible to estimate the complete particle-size distribution from the sand, silt, and clay fractions, then what are the minimal data that are required?

In this paper we report a simple method for estimating the particle-size distribution from the fractions of clay, silt, and one sand subclass, the fine plus very fine sand fraction (particle radii between 25 and 125 μm). The method is easy to use, with the estimated distribution being defined completely by Eq. [4], an expression that depends explicitly on the clay, silt, and fine plus very fine sand fractions.

THEORY

We describe the soil cumulative particle-size distribution using the following empirical model:

$$P(r) = \frac{1}{1 + (1/P(r_0) - 1)\exp(-uR^c)}, \qquad [1a]$$

$$R = \frac{r - r_0}{r_0}, \qquad r \geq r_0 > 0. \qquad [1b]$$

In Eq. [1], $P(r)$ is the mass fraction of soil particles with radii less than r, r_0 is the lower bound on radii for which the model applies, and c and u are model parameters. Equation [1] is similar to a logistic growth curve (e.g., Thornley, 1990) except for the additional parameter c. As a descriptor of soil particle-size distributions, several things are noteworthy about Eq. [1]. First, the model describes the distribution only for $r > r_0 > 0$, and it is necessary to specify the value of the distribution at r_0, $P(r_0) > 0$. Second, the model dictates $P(r_2) > P(r_1)$ for any $r_2 > r_1$, which may not be consistent with an exceptionally poorly graded soil. Finally, the model predicts $P \rightarrow 1$ as $r \rightarrow$

George E. Brown, Jr. Salinity Lab., 450 W. Big Springs Rd., Riverside, CA 92507. Received 24 July 2000. *Corresponding author (tskaggs@ussl.ars.usda.gov).

Published in Soil Sci. Soc. Am. J. 65:1038–1044 (2001).

Abbreviations: cl, clay fraction; fvfs, fine plus very fine sand fraction; si, silt fraction.

∞, meaning it cannot be guaranteed that $P \rightarrow 1$ at the upper limit of soil material as it should (i.e., at $r = 1000$ μm in the USDA soil particle-size classification system). Nevertheless, we have found Eq. [1] to be a flexible and useful model for describing the particle-size distribution.

The basis of our estimation method is that Eq. [1] can be rearranged so it is linear with slope c and intercept ln u,

$$\ln u + c\ln\frac{r - r_0}{r_0} = \ln\left[-\ln\frac{1/P(r) - 1}{1/P(r_0) - 1}\right] (r > r_0) \quad [2]$$

The linearity means that given $P(r_0)$ plus two additional values of the particle-size distribution, $P(r_1)$ and $P(r_2)$, we can write two equations that may be solved to calculate the two unknown parameters, c and u. The resulting expressions for c and u are

$$c = \alpha\ln\frac{v}{w} \quad [3a]$$

and

$$u = -v^{1-\beta}w^{\beta}, \quad [3b]$$

where

$$v = \ln\frac{1/P(r_1) - 1}{1/P(r_0) - 1}, \qquad w = \ln\frac{1/P(r_2) - 1}{1/P(r_0) - 1}, \quad [3c]$$

$$\alpha = 1/\ln\frac{r_1 - r_0}{r_2 - r_0}, \qquad \beta = \alpha\ln\frac{r_1 - r_0}{r_0}, \quad [3d]$$

$$1 > P(r_2) > P(r_1) > P(r_0) > 0, \quad r_2 > r_1 > r_0 > 0. \quad [3e]$$

Thus we can use Eq. [1] to model the particle-size distribution with parameters c and u being determined entirely by $P(r_2)$, $P(r_1)$, and $P(r_0)$ as specified in Eq. [3]. Note from Eq. [3c] that v and w are negative numbers because the arguments of the logarithms are less than one; recall $P(r_1) > P(r_0)$, and $P(r_2) > P(r_0)$. Equation [3b] therefore contains two negative quantities being raised to the powers $1 - \beta$ and β, respectively, suggesting the undesirable possibility that u is complex for non-integer values of β. However, it can be seen that u is real by noting that since $v < 0$ and $w < 0$,

$$\begin{aligned} u &= -v^{1-\beta}w^{\beta}, \\ &= -(-|v|)^{1-\beta}(-|w|)^{\beta}, \\ &= -(-1)^{1-\beta}|v|^{1-\beta}(-1)^{\beta}|w|^{\beta}, \\ &= |v|^{1-\beta}|w|^{\beta}, \end{aligned}$$

which is positive and real for any real β. Nevertheless, numerically calculating u based on Eq. [3b] may yield $u' = u + iy$, where $i = \sqrt{-1}$ and y is very close to zero. In this case, use the real part of the computed value, $\mathrm{Re}(u') = u$, as the parameter in Eq. [1]. Alternatively, one may compute u by either of the following equivalences,

$$u = (-v)^{1-\beta}\,(-w)^{\beta} = |v|^{1-\beta}|w|^{\beta},$$

neither of which lead to problems with complex numbers.

MATERIALS AND METHODS

Particle-Size Distribution Estimation

To implement the method described in the above section, we must select values for r_0, r_1, and r_2. In this work we use $r_0 = 1$ μm, $r_1 = 25$ μm, and $r_2 = 125$ μm. According to the particle-size classification system shown in Fig. 1, these radii specify that $P(r_0)$ is the clay mass fraction (cl), $P(r_1)$ is the clay plus silt fraction (cl + si), and $P(r_2)$ is the clay plus silt plus fine sand plus very fine sand mass fraction (cl + si + fs + vfs). Note that we do not need to know both the fine and very fine sand fractions, only their sum (fvfs = fs + vfs).

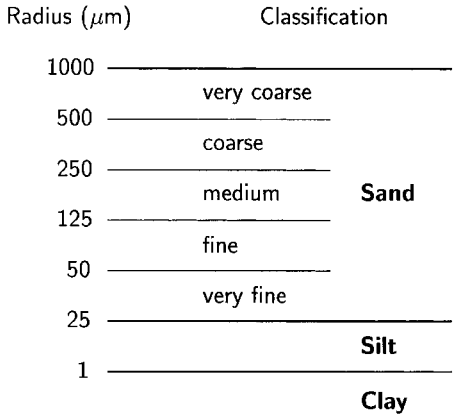

Fig. 1. Particle-size classification system used in this study. The system differs from the USDA system only in that particle-size is expressed in terms of the particle radius (instead of diameter) and the units are micrometers (instead of mm).

Substituting these radii and definitions into Eq. [1] and [3] yields the following expression for the estimated particle-size distribution:

$$\tilde{P}(r; \mathrm{cl}, \mathrm{si}, \mathrm{fvfs}) = \frac{1}{1 + (1/\mathrm{cl} - 1)\exp\left[-u(r - 1)^c\right]}, \quad 1\ \mu\mathrm{m} \le r \le 1000\ \mu\mathrm{m}, \quad [4a]$$

where

$$c = -.609\ln\frac{v}{w}, \qquad u = -\frac{v^{2.94}}{w^{1.94}}, \quad [4b]$$

$$v = \ln\frac{(\mathrm{cl} + \mathrm{si})^{-1} - 1}{\mathrm{cl}^{-1} - 1}, \qquad w = \ln\frac{(\mathrm{cl} + \mathrm{si} + \mathrm{fvfs})^{-1} - 1}{\mathrm{cl}^{-1} - 1}. \quad [4c]$$

In Eq. [4] we introduce the symbol $\tilde{P}$ to indicate the model particle-size distribution that is "estimated" when u and c are determined from the minimal texture data cl, si, and fvfs (i.e., three data points). Later, we contrast this estimated distribution with the "fitted" model distribution that is obtained when u and c are determined by fitting Eq. [1] to abundant data (i.e., >10 data points).

Particle-Size Data

To test the accuracy of Eq. [4], we compiled 125 measured particle-size distributions. Forty-nine of the measured distributions were for soils sampled during the SGP-97 Hydrology Experiment (Shouse, P.J., B.P. Mohanty, D.A. Miller, J.A. Jobes, J. Fargerlund, W.B. Russell, T.H. Skaggs, and M.Th. van Genuchten. 2001. Soil properties of dominant soil types of the southern great plains 1997 (SGP97) hydrology experiment. Unpublished USDA Salinity Laboratory report. See also http://hydrolab.arsusda.gov/sgp97/). The SGP-97 soils are from central Oklahoma, and the method of particle-size measurement was a combination of wet sieving and the hydrometer method (Gee and Bauder, 1986). Fifty-seven of the 125 measured distributions were taken from the UNSODA database (Leij et al., 1996). The UNSODA soils are from locations around the world and the methods used in the particle-size

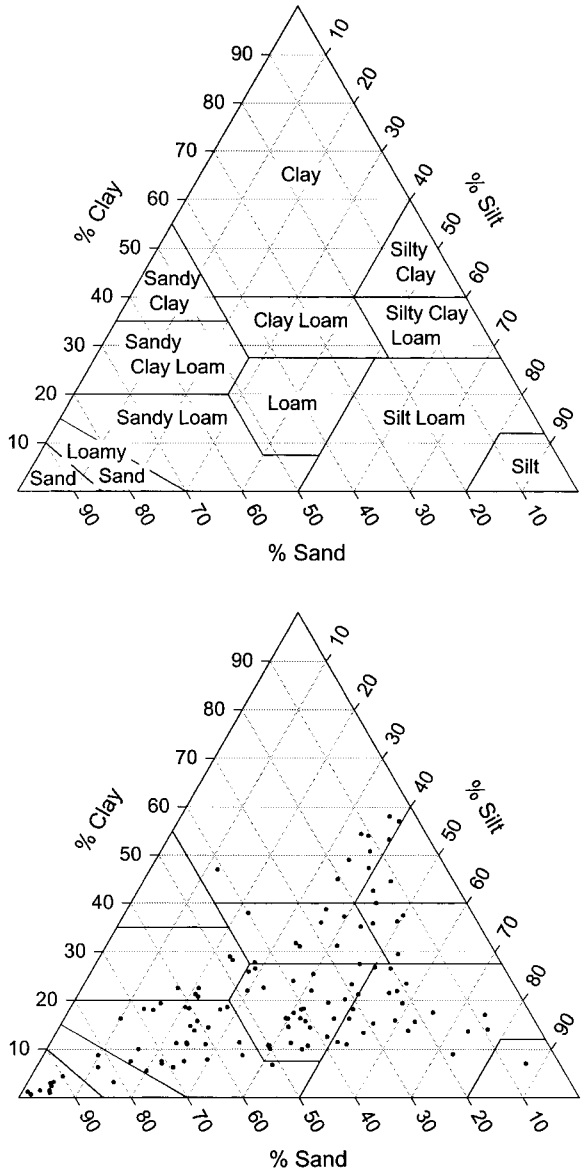

Fig. 2. The USDA soil texture classification system (top) and the range of soil textures covered in this study (bottom).

measurements varied, but all involved some combination of sieving and either the hydrometer method or the pipette method (Gee and Bauder, 1986). The remaining 19 soils were from various locations in California, and the measurement protocol was the same as for the SGP-97 soils. Figure 2 shows the range of soil textures covered by the 125 soils.

The particle-size data consist of measurements of the particle-size distribution at discrete values of the particle radius. The number of measurements for each soil ranged from $n = 17$ to $n = 21$. We denote the set of radii for which there is a measurement as $\hat{r}_j$, $j = 1...n$, and the measured cumulative mass fraction at $\hat{r}_j$, as $\hat{P}(\hat{r}_j)$. The necessary inputs for Eq. [4] are then given by

$$\text{cl} = \hat{P}(1\ \mu\text{m}) \quad [5a]$$

$$\text{si} = \hat{P}(25\ \mu\text{m}) - \text{cl}, \quad [5b]$$

$$\text{fvfs} = \hat{P}(125\ \mu\text{m}) - \text{cl} - \text{si}, \quad [5c]$$

where straight-line interpolation between data points was used when there was no measurement at exactly 1, 25, or 125 μm.

The 125 data sets were evaluated for compliance with Eq. [3e]. In the context of Eq. [4], Eq. [3e] requires $0 < \text{cl} < \text{cl} + \text{si} < \text{cl} + \text{si} + \text{fvfs} < 1$. Three of the soils (a clay, a silt loam, and a silty clay loam) failed to meet this criterion because $\text{cl} + \text{si} + \text{fvfs} = 1$ (i.e., there were no soil particles with radii >125 μm). So that these three soils could be included in our analysis, we reduced their fvfs fraction by a tenth of one percent, $\text{fvfs}' = \text{fvfs} - 0.001$, and used fvfs′ in Eq. [4] in place of fvfs.

Goodness-of-Fit

We use two goodness-of-fit measures to evaluate the accuracy of Eq. [4], the average absolute deviation (AAD),

$$\text{AAD}_{\tilde{P}} = \frac{1}{n}\sum_{j=1}^{n}|\tilde{P}(\hat{r}_j) - \hat{P}(\hat{r}_j)|\,, \quad 1\ \mu\text{m} \le \hat{r}_j \le 1000\ \mu\text{m}, \quad [6]$$

and the maximum absolute deviation (MAD),

$$\text{MAD}_{\tilde{P}} = \max_{1\le j\le n}|\tilde{P}(\hat{r}_j) - \hat{P}(\hat{r}_j)|,\ 1\ \mu\text{m} \le \hat{r}_j \le 1000\ \mu\text{m}. \quad [7]$$

We also want to evaluate the accuracy of Eq. [4] relative to the fit that is achieved when Eq. [1] is fitted to each of the 125 measured distributions. The reason is that this allows us to assess which inaccuracies in $\tilde{P}$ are due to the use of limited data and which are due to the fact that the generalized logistic model may be a poor representation of a particular particle-size distribution. The fitted distribution is

$$P(r; u, c) = \frac{1}{1 + (1/\text{cl} - 1)\exp\left[-u(r-1)^c\right]}, \quad 1\ \mu\text{m} \le r \le 1000\ \mu\text{m}, \quad [8a]$$

where u and c minimize the nonlinear least-square objective function,

$$\min\ \Phi(u, c) = \sum_{j=1}^{n}[P(\hat{r}_j; u, c) - \hat{P}(\hat{r}_j)]^2 \quad 1\ \mu\text{m} \le \hat{r}_j \le 1000\ \mu\text{m}. \quad [8b]$$

Equation [8b] was minimized using *Mathematica*'s FindMinimum function (Wolfram, 1999). The goodness-of-fit measures for the fitted distribution are given by

$$\text{AAD}_P = \frac{1}{n}\sum_{j=1}^{n}|P(\hat{r}_j) - \hat{P}(\hat{r}_j)|, \quad 1\ \mu\text{m} \le \hat{r}_j \le 1000\ \mu\text{m}, \quad [9]$$

and

$$\text{MAD}_P = \max_{1\le j\le n}|P(\hat{r}_j) - \hat{P}(\hat{r}_j)|, \quad 1\ \mu\text{m} \le \hat{r}_j \le 1000\ \mu\text{m}. \quad [10]$$

RESULTS AND DISCUSSION

Figure 3 shows estimated and fitted distributions for selected particle-size distributions. Table 1 contains parameter and goodness-of-fit values for each of the plots in Fig. 3. In Fig. 3a through 3d, the estimated distributions ($\tilde{P}$) are in good agreement with the data and are very similar to the fitted distributions (P). Values of $\text{AAD}_{\tilde{P}}$ for these plots range from 0.49 to 1.3%, while $\text{MAD}_{\tilde{P}}$ ranges from 1.5 to 7.6% (Table 1). The range

Table 1. Parameter and goodness-of-fit values for Fig. 3.†

				Estimated, $\tilde{P}$				Fitted, P			
Fig.	cl	si	fvfs	u	c	$AAD_{\tilde{P}}$	$MAD_{\tilde{P}}$	u	c	AAD_P	MAD_P
						%				%	
3a	0.226	0.324	0.347	0.27	0.52	0.62	1.5	0.26	0.54	0.61	1.3
3b	0.044	0.056	0.55	0.055	0.87	0.49	3.1	0.046	0.91	0.5	1.3
3c	0.032	0.153	0.8	0.14	0.83	1.3	5.8	0.11	0.89	1.3	2.8
3d	0.372	0.395	0.229	0.14	0.79	1.0	7.6	0.18	0.69	1.1	4.7
3e	0.088	0.355	0.387	0.64	0.38	5.2	14.0	0.51	0.45	4.9	11.0
3f	0.225	0.208	0.565	0.018	1.3	3.0	19.0	0.045	0.96	1.4	6.6
3g	0.194	0.588	0.211	0.5	0.53	4.1	20.0	0.093	1.1	1.2	4.3
3h	0.07	0.87	0.048	3.2	0.16	13.0	60.0	0.27	0.96	1.3	3.9

† cl, clay; si, silt; fvfs, fine plus very fine sand. AAD and MAD are the average and maximum absolution deviations, respectively. u and c are model parameters.

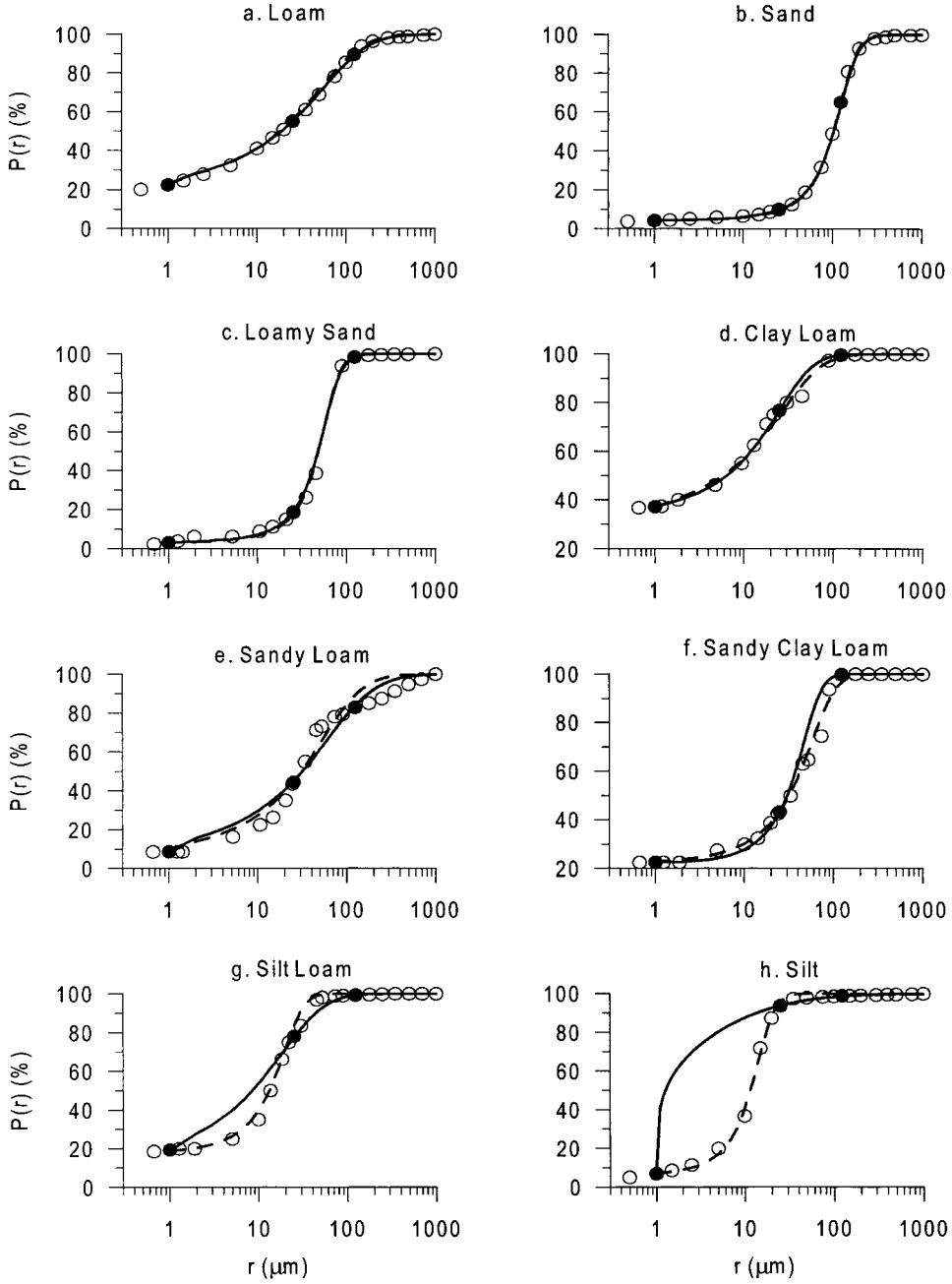

Fig. 3. Estimated and fitted distributions for selected particle-size data. In each plot, the solid line is the estimate $\tilde{P}$ given by Eq. [4] and the dashed line is the fitted distribution P defined by Eq. [8]. The circles are the measured particle-size data, with the three filled circles in each plot corresponding to the values used as input in Eq. [4]: cl, cl + si, and cl + si + fvfs. Table 1 contains parameter and goodness-of-fit values for each plot. cl, clay fraction; fvfs, fine plus very fine sand fraction; si, silt fraction.

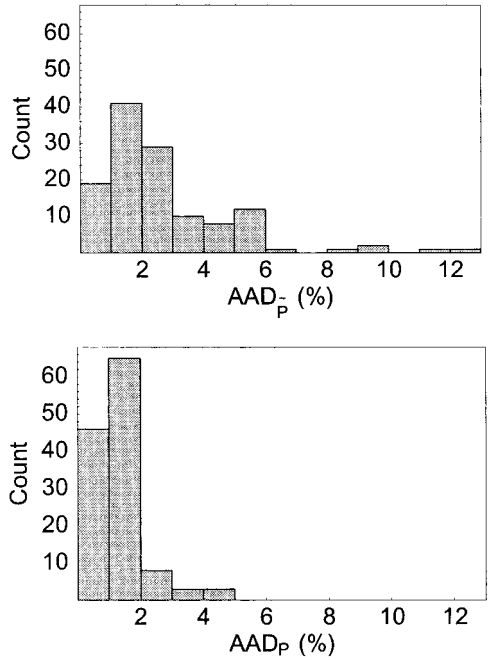

Fig. 4. Histograms of the average absolute deviations AAD$_P$ (top) and AAD$_P$ (bottom).

for AAD$_P$ is essentially the same (0.5–1.1%), whereas MAD$_P$ ranges from 1.3 to 4.7%. In Fig. 3e, discrepancies between $\tilde{P}$ and the data are partially attributable to the generalized logistic equation not being a good model of the poorly graded data, a failing that would be expected with any simple two-parameter distribution model. In this case the fitted distribution (AAD$_P$ = 4.9%, MAD$_P$ = 11%) is only marginally better than the estimated distribution (AAD$_{\tilde{P}}$ = 5.2%, MAD$_{\tilde{P}}$ = 14%). Figures 3f through 3h show cases where $\tilde{P}$ deviates from both the data and P, with AAD$_{\tilde{P}}$ ranging from 3 to 13%, AAD$_P$ ranging from 1.2 to 1.4%, MAD$_{\tilde{P}}$ ranging from 19 to 60%, and MAD$_P$ ranging from 3.9 to 6.6%.

While it is evident from Fig. 3 that the accuracy of $\tilde{P}$ varied, those examples were selected to illustrate a range of soil textures and the range of AAD$_{\tilde{P}}$ and MAD$_{\tilde{P}}$ values that were observed, and they are not indicative of the proportion of good and bad estimates that were obtained. The goodness-of-fit results for all 125 soils are shown as histograms in Fig. 4 and 5. Figure 4 shows that AAD$_{\tilde{P}}$ was less than 2% for 60 soils and less than 4% for 99 soils. In comparison, AAD$_P$ was less than 2% for 111 soils and less than 4% for 122 soils (Fig. 4.). Fitting never resulted in AAD$_P$ being greater than 5%, whereas estimation by Eq. [4] resulted in AAD$_{\tilde{P}}$ being greater than 5% in 18 cases. Figure 5 paints a similar picture for MAD, with estimation by Eq. [4] finding 66 cases with MAD$_P$ less that 10%, and fitting of Eq. [8] finding 120 cases with MAD$_{\tilde{P}}$ less than 10%. The results for the three soils with the adjusted fine plus very fine sand fraction (fvfs′) were unremarkable, all having AAD$_{\tilde{P}}$ values less than 2% and MAD$_{\tilde{P}}$ values less than 10%.

As one would expect, there is a loss of accuracy involved in going from fitting the full distribution to estimating the distribution based on only cl, si, and fvfs. While the question of whether or not $\tilde{P}$ is sufficiently accurate will depend on the intended use of the estimated distribution, it is evident from Fig. 3 through 5 that a handful of the estimated distributions are extremely poor, with AAD$_{\tilde{P}}$ greater than 6%, MAD$_{\tilde{P}}$ greater than 30%, and an estimated distribution that has an incorrect curvature (Fig. 3h). Figure 6 demonstrates that these extremely poor predictions occurred when the silt fraction was greater than about 70%. We therefore recommend that Eq. [4] be used only when si is less than 0.7.

It is instructive to view the results shown in Fig. 3 when plotted according to the linear relationship that

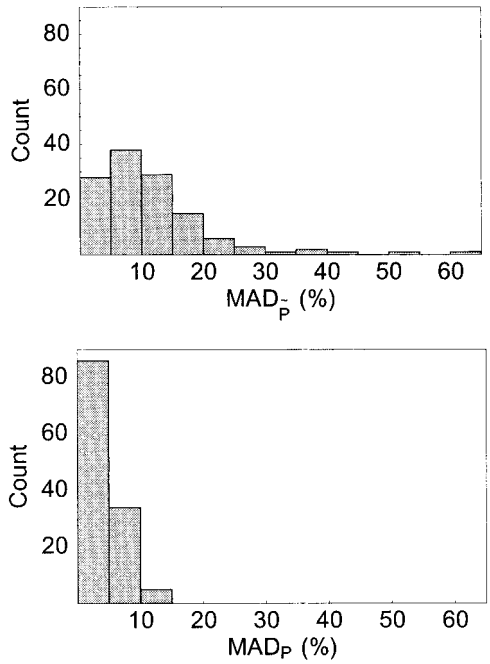

Fig. 5. Histograms of the maximum absolute deviations MAD$_P$ (top) and MAD$_P$ (bottom).

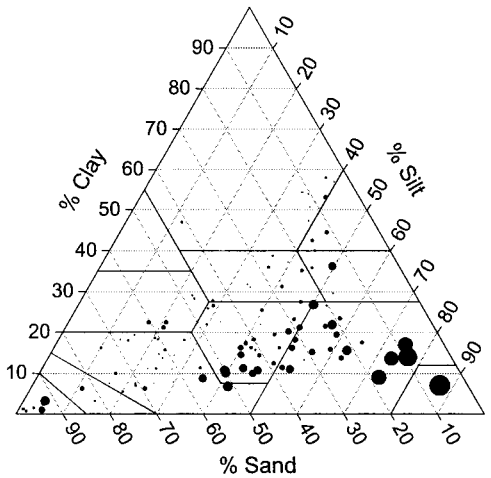

Fig. 6. Illustration of the average absolute deviation (AAD$_P$) obtained for each soil. The size of a point is proportional to AAD$_P$, with the largest value being AAD$_P$ = 12.8%. The plot demonstrates that $\tilde{P}$ was a poor estimate of the particle-size distribution whenever the silt mass fraction was greater than about 70%.

is indicated in Eq. [2]. In Fig. 7, the y-axes are the right-hand side of Eq. [2] and the x-axes are $\ln[(r - r_0)/r_0]$. In this frame of reference, the estimated and fitted model distributions are lines with slope c and intercept $\ln u$, where c and u are the parameters given in Table 1. Note that the fitted parameter values are based on the nonlinear fit defined in Eq. [8] and not a linear regression to the data in Fig. 7. In contrast to Fig. [3], the cl data point used by Eq. [4] is not shown in Fig. 7 because data can be plotted only for $r > r_0$. Figure 7h shows that for the silt soil $\tilde{P}$ is a poor estimate because there is very little soil in the fine plus very fine sand fraction and therefore the cl + si + fvfs data point provides almost no information about the distribution.

Other choices for r_0, r_1, and r_2 are possible. We tested $r_2 = 50$ μm, which makes $P(r_2)$ equal to the clay plus silt plus very fine sand fraction. The results obtained were comparable for many of the soils, but were significantly worse for others, particularly sands. Overall, the results obtained using $r_2 = 125$ μm were judged superior.

Since Eq. [4] is intended for cases where the full distribution is not known, the remaining pertinent question is: What accuracy is expected for some arbitrarily chosen soil (with si < 0.7)? We cannot answer this ques-

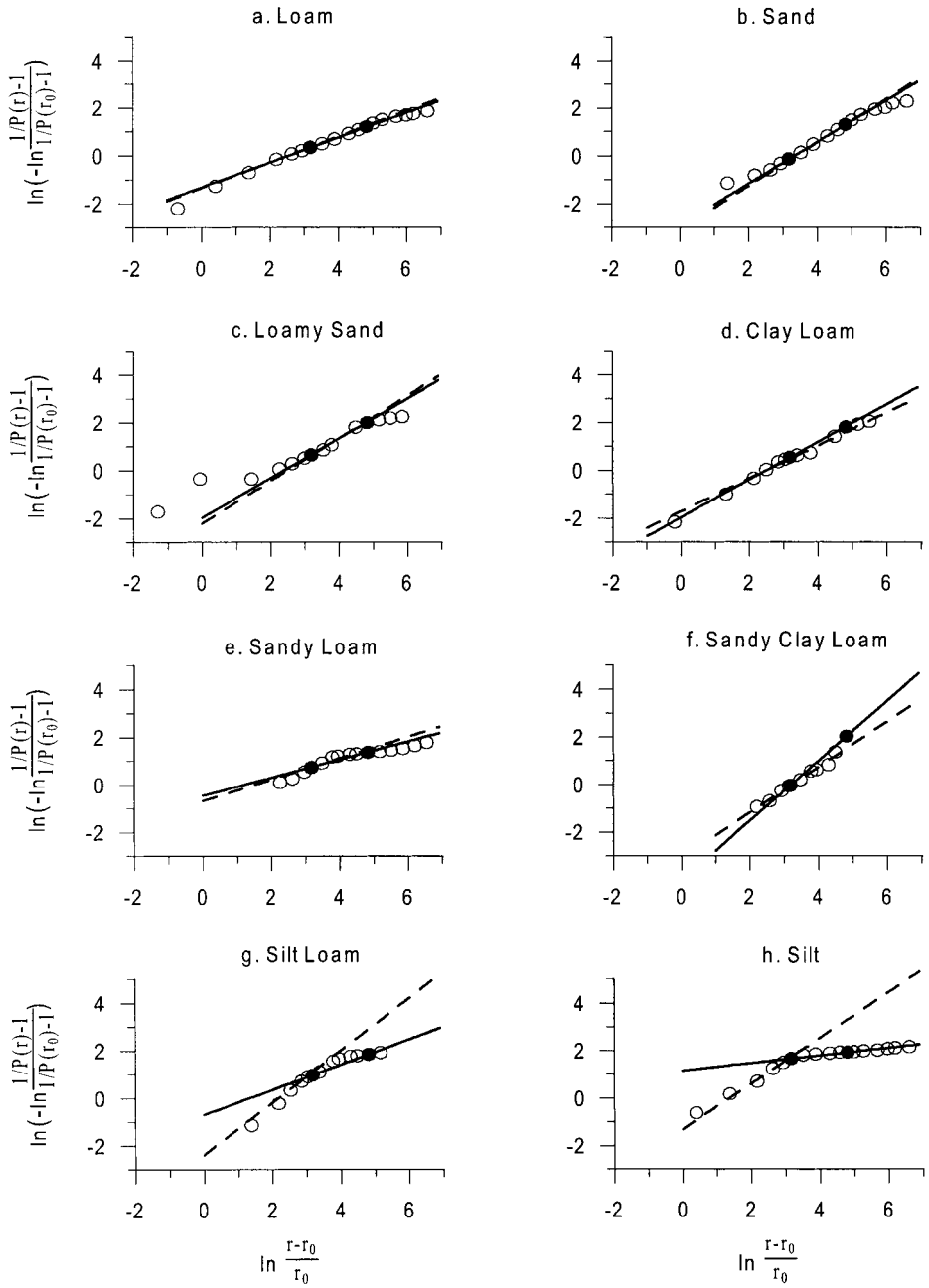

Fig. 7. The data and model distributions from Fig. 3 replotted to illustrate the linear relationship that is indicated by Eq. [2]. In these plots data can be shown only for $r > r_0$ and $P(r) < 1$. The two filled circles in each plot correspond to the cl + si and cl + si + fvfs values used as input in Eq. [4]. cl, clay fraction; fvfs, fine plus very fine sand fraction; si, silt fraction.

tion definitively because our test data set was not exhaustive. Nevertheless, we note that the median $AAD_{\tilde{P}}$ was 2% (excluding the 5 soils with si > 0.7), and the median $AAD_{\hat{P}}$ was 8.9%. Thus, based on our data set, we expect that the absolute deviation of the estimated distribution from the true distribution, $|\tilde{P}(r) - \hat{P}(r)|$, will typically average 0.02 over 1 μm $\leq r \leq$ 1000 μm, and be nowhere greater than 0.09. Corresponding upper bounds on these errors are approximately 0.06 for the average deviation and 0.3 for the maximum deviation.

SUMMARY AND CONCLUSIONS

The objective of this study was to devise a method for estimating the soil particle-size distribution when only a few particle-size data are available. Using a generalized logistic model, we presented a method in which the distribution is estimated from only the clay mass fraction (cl), the silt mass fraction (si), and the fine plus very fine sand mass fraction (fvfs). The estimated distribution is given by Eq. [4], a relatively simple expression.

The accuracy of the estimation method was evaluated using 125 measured particle-size distributions. We found that the estimation method should not be used when the silt fraction is greater than about 0.7. For the remaining 120 soils, the estimated distributions ranged from exceptionally good (e.g., Fig. 3a) to reasonably good (e.g., Fig. 3e). More quantitatively, we observed that the average absolute deviation of the estimated distribution from the data was less than 4% in 99 of 120 soils, and that the maximum absolute deviation was less than 10% in 66 of 120 soils. For all 120 soils the median level of accuracy corresponded to an average absolute deviation of 2% and a maximum absolute deviation of 9%. The observed upper bound for these errors was approximately 6% for the average deviation and 30% for the maximum deviation.

Ideally, the complete particle-size distribution should be measured and reported when mapping soil physical properties. Short of this, the next preference would be for measurements of the clay and silt fractions, plus all sand subclasses. In some survey work, time and labor constraints may limit measurements to only the percentages of sand, silt, and clay. Our findings suggest that considerable benefit would be realized if these minimal data were expanded to include one sand subdivision, such as the fine plus very fine sand fraction.

ACKNOWLEDGMENTS

This study was partially supported by NASA Land Surface Hydrology grant #NAG5-8682. This article also benefited from the comments and suggestions of three anonymous reviewers.

REFERENCES

Arya, L.M., F.J. Leij, M.Th. van Genuchten, and P.J. Shouse. 1999. Scaling parameter to predict the soil water characteristic from particle-size distribution data. Soil Sci. Soc. Am. J. 63:510–519.

Bittelli, M., G.S. Campbell, and M. Flury. 1999. Characterization of particle-size distribution in soils with a fragmentation model. Soil Sci. Soc. Am. J. 63:782–788.

Crawford, J.W., B.D. Sleeman, and I.M. Young. 1993. On the relation between number-size distributions and the fractal dimension of aggregates. J. Soil Sci. 44:555–565.

Gee, G.W., and J.W. Bauder. 1986. Particle-size analysis. p. 383–411. *In* A. Klute (ed.) Methods of soil analysis. Part 1. 2nd ed. Agron. Monogr. 9. ASA and SSSA, Madison, WI.

Kozak, E., Ya.A. Pachepsky, S. Sokolowski, Z. Sokolowska, and W. Stepniewski. 1996. A modified number-based method for estimating fragmentation fractal dimensions of soils. Soil Sci. Soc. Am. J. 60:1291–1297.

Leij, F.J., W.J. Alves, M.Th. van Genuchten, and J.R. Williams. 1996. The UNSODA unsaturated soil hydraulic database user's manual. Version 1.0. Tech. Rep. EPA/600/R-96/095. U.S. EPA, Cincinnati, OH.

Nemes, A., J.H.M. Wösten, A. Lilly, and J.H. Oude Voshaar. 1999. Evaluation of different procedures to interpolate particle-size distributions to achieve compatibility with soil databases. Geoderma 90:187–202.

Shirazi, M.A., L. Boersma, and J.W. Hart. 1988. A unifying quantitative analysis of soil texture: Improvement of precision and extension of scale. Soil Sci. Soc. Am. J. 52:181–190.

Taguas, F.J., M.A. Martín, and E. Perfect. 1999. Simulation and testing of self-similar structures for soil particle-size distributions using iterated function systems. Geoderma 88:191–203.

Thornley, J.H.M. 1990. A new formulation of the logistic growth equation and its application to leaf area growth. Ann. Bot. 66:309–311.

Turcotte, D.L. 1986. Fractals and fragmentation. J. Geophys. Res. 91: 1921–1926.

Tyler, S.W., and S.W. Wheatcraft. 1992. Fractal scaling of soil particle-size distributions: Analysis and limitations. Soil Sci. Soc. Am. J. 56:362–369.

Wolfram, S. 1999. The mathematica book. Cambridge University Press, New York.